

Enhanced magnetoelectric effect in heterostructure of magnetostrictive alloy bars and piezoelectric single-crystal transformer

Chung Ming Leung, Siu Wing Or, Feifei Wang, S. L. Ho, and Haosu Luo

Citation: *Rev. Sci. Instrum.* **82**, 013903 (2011); doi: 10.1063/1.3529439

View online: <http://dx.doi.org/10.1063/1.3529439>

View Table of Contents: <http://rsi.aip.org/resource/1/RSINAK/v82/i1>

Published by the [American Institute of Physics](#).

Related Articles

Micro-fabrication process for small transport devices of layered manganite

J. Appl. Phys. **111**, 07E129 (2012)

Electrical properties of magnetic nanocontact devices computed using finite-element simulations

Appl. Phys. Lett. **100**, 083507 (2012)

High power and low critical current spin torque oscillation from a magnetic tunnel junction with a built-in hard axis polarizer

Appl. Phys. Lett. **100**, 032405 (2012)

Gauge fields in spintronics

App. Phys. Rev. **2011**, 17 (2011)

Gauge fields in spintronics

J. Appl. Phys. **110**, 121301 (2011)

Additional information on Rev. Sci. Instrum.

Journal Homepage: <http://rsi.aip.org>

Journal Information: http://rsi.aip.org/about/about_the_journal

Top downloads: http://rsi.aip.org/features/most_downloaded

Information for Authors: <http://rsi.aip.org/authors>

ADVERTISEMENT



Enhanced magnetoelectric effect in heterostructure of magnetostrictive alloy bars and piezoelectric single-crystal transformer

Chung Ming Leung,¹ Siu Wing Or,^{1,a)} Feifei Wang,² S. L. Ho,¹ and Haosu Luo³

¹*Department of Electrical Engineering, The Hong Kong Polytechnic University, Hung Hom, Kowloon, Hong Kong*

²*Key Laboratory of Optoelectronic Material and Device, Mathematics and Science College, Shanghai Normal University, Shanghai 200234, China*

³*Information Materials and Devices Research Center, Shanghai Institute of Ceramics, Chinese Academy of Sciences, Shanghai 201800, China*

(Received 22 July 2010; accepted 28 November 2010; published online 19 January 2011)

We report an enhanced magnetoelectric (ME) effect in a heterostructure consisting of a long-type, longitudinally–longitudinally polarized $0.71\text{Pb}(\text{Mg}_{1/3}\text{Nb}_{2/3})\text{O}_3$ – 0.29PbTiO_3 (PMN–PT) piezoelectric single-crystal transformer with its input part sandwiched between two longitudinally magnetized $\text{Tb}_{0.3}\text{Dy}_{0.7}\text{Fe}_{1.92}$ (Terfenol-D) magnetostrictive alloy bars. The observed ME effect has two independent operational modes: namely, ME sensing mode and ME transduction mode. The ME sensing mode features a large ME voltage coefficient (α_V) of ~ 0.32 V/Oe over a flat frequency range of 1–50 kHz, while the ME transduction mode possesses two colossal resonance α_V of 7.6 and 7.9 V/Oe, corresponding to the first and second longitudinal resonances, at 56.2 and 127.9 kHz, respectively. This enhanced dual-mode ME effect not only enables the application potential of the heterostructure, but also advances the technology of power-free ME sensors and transducers. © 2011 American Institute of Physics. [doi:10.1063/1.3529439]

I. INTRODUCTION

The magnetoelectric (ME) effect in materials which are simultaneously ferromagnetic and ferroelectric has attracted great research interest in the past decade because of the ability to convert energy between magnetic and electric forms for a broad domain of applications such as magnetic field sensors, electric current sensors, ME transducers, filters, resonators, etc.^{1–4} While the ME effect was first observed in single-phase materials such as Cr_2O_3 , the inherently weak ME coupling and the complex synthesis process impede the application viability of the materials.^{5–8} By contrast, multiphase laminated composites based on magnetostrictive and piezoelectric materials have resulted in practically useable extrinsic ME effect characterized by large ME voltage coefficients ($\alpha_V = dV/dH$) in excess of 20 mV/Oe over broad ranges of frequency (> 20 kHz) and temperature ($> 60^\circ\text{C}$).^{6,9–12} In fact, a variety of ME configurations and composite shapes have been studied, including longitudinally or transversely magnetized, longitudinally or transversely polarized composite plates; radially or axially magnetized, radially or axially polarized composite disks; circumferentially magnetized, axially polarized composite rings, etc.^{9–17}

Recent evolution in magnetoelectricity has a main focus on enhancing α_V and other operational parameters while increasing the multifunctionality of the materials for advanced sensor and transducer applications. By combining a classical Rosen-type piezoelectric transformer as shown in Fig. 1 with a traditional ME laminated composite or a magnetostrictive alloy, it can achieve an improved ME energy conversion under resonance conditions.^{14,18} However, this classical Rosen-

type piezoelectric transformer suffers intrinsically from: (1) difficulty in imparting two orthogonal polarizations in the transverse and longitudinal directions for the input and output parts, respectively; (2) residual stress concentration-induced mechanical breakdown in the central portion between the input and output parts with orthogonal polarization directions; (3) complex transverse and longitudinal modes of operation; and (4) acoustic mismatch between the input and output parts.^{19–21}

In this work, we propose an enhanced ME effect in a novel heterostructure formed by bonding two longitudinally magnetized $\text{Tb}_{0.3}\text{Dy}_{0.7}\text{Fe}_{1.92}$ (Terfenol-D) magnetostrictive alloy bars to the input part of a long-type, longitudinally–longitudinally polarized $0.71\text{Pb}(\text{Mg}_{1/3}\text{Nb}_{2/3})\text{O}_3$ – 0.29PbTiO_3 (PMN–PT) piezoelectric single-crystal transformer. The proposed effect gives two interesting and independent operational modes in the heterostructure, including a first ME sensing mode in a broad frequency range of 1–50 kHz and a second ME transduction mode associated with the enhanced first and second shape (longitudinal) resonances by the PMN–PT transformer. The reasons of using the specific long-type piezoelectric transformer instead of the classical Rosen-type piezoelectric transformer (Fig. 1) are that: (1) it allows the two longitudinal polarizations of the same direction for the input and output parts; (2) it releases residual stress concentration imposed by different polarization directions; (3) it has pure longitudinal mode of operation; and (4) it provides an improved acoustic match between the input and output parts.²²

II. EXPERIMENTAL DETAILS

Figure 2 shows the schematic diagram of the proposed heterostructure based on a long-type PMN–PT transformer

^{a)} Author to whom correspondence should be addressed. Electronic mail: eeswor@polyu.edu.hk.

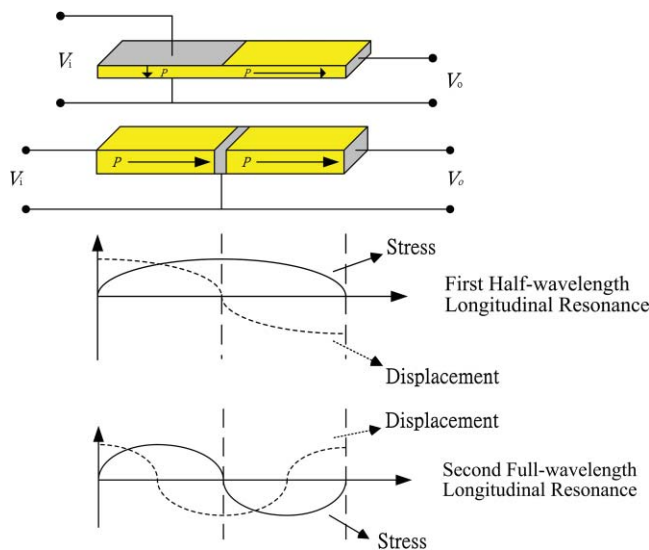


FIG. 1. (Color online) Schematic diagrams showing the classical Rosen-type piezoelectric transformer, the long-type piezoelectric transformer, and the displacement and stress distributions along the length of the transformers for the first (half-wavelength) and second (full-wavelength) longitudinal resonances. The labels V_i and V_o denote the input and output voltages of the transformers, respectively.

and two Terfenol-D bars. The PMN-PT transformer was cut from a PMN-PT ingot grown in-house using a modified Bridgman method to have dimensions and crystallographic orientations of $16[100]^L \times 2[011]^W \times 2[0\bar{1}1]^H \text{ mm}^3$, where L is the length, W is the width, and H is the height.^{22,23} Silver paste was applied to the two main end surfaces normal to the longitudinal (or 3-) direction to form the ME sensing mode electrode (labeled with $V_{\text{ME,S}}$) and the ME transduction mode electrode (labeled with $V_{\text{ME,T}}$) as well as on the four side surfaces covering the central 2 mm portion normal to the transverse (or 1-, 2-) directions to form the ground electrode. After firing the silver paste electrodes at 650 °C for 1 h, two polarizations of the same direction were induced in

the PMN-PT transformer along the longitudinal direction for the input and output parts using a dc voltage of 4 kV at 115 °C for 15 min followed by a reduced dc voltage of 2 kV in a natural cooling run to room temperature in a silicon oil bath. The Terfenol-D bars were commercially supplied (Baotou Rare Earth Research Institute, China) to have dimensions of $6^L \times 2^W \times 2^H \text{ mm}^3$ and their highly magnetostrictive [112] crystallographic axis oriented along the longitudinal direction. To fabricate the heterostructure, the surface-cleaned Terfenol-D bars were adhered symmetrically to the input part of the PMN-PT transformer using an insulating epoxy adhesive, and the heterostructure was pressed at 8 MPa while cured at 40 °C for 6 h to achieve good mechanical coupling.

The working principles of the heterostructure can be described by an ME sensing mode and an ME transduction mode. In the ME sensing mode, the magnetostrictive effect in the Terfenol-D bars is mediated mechanically with the piezoelectric effect in the input part of the PMN-PT transformer. The ME configuration of this mode is an analogy to a longitudinally magnetized, longitudinally polarized ME laminated composite.²⁴ In the ME transduction mode, the resonance magnetostrictive effect in the Terfenol-D bars is mediated mechanically with the resonance piezoelectric effect in the PMN-PT transformer. In more details, an ac magnetic field (H_3) applied along the longitudinal direction of the heterostructure leads to longitudinal vibrations of the Terfenol-D bars. These longitudinal vibrations, in turn, couple mechanically to the input part of the PMN-PT transformer, causing it to produce a piezoelectric voltage ($V_{\text{ME,S}}$) at the ME sensing mode electrode with respect to the ground. In the meantime, these longitudinal vibrations are transferred to the output part of the PMN-PT transformer and, under resonance conditions, gain an effective amplification, resulting in an amplified piezoelectric voltage ($V_{\text{ME,T}}$) at the ME transduction mode electrode with respect to the ground.

The ME effect in the fabricated heterostructure was characterized using an in-house automated measurement

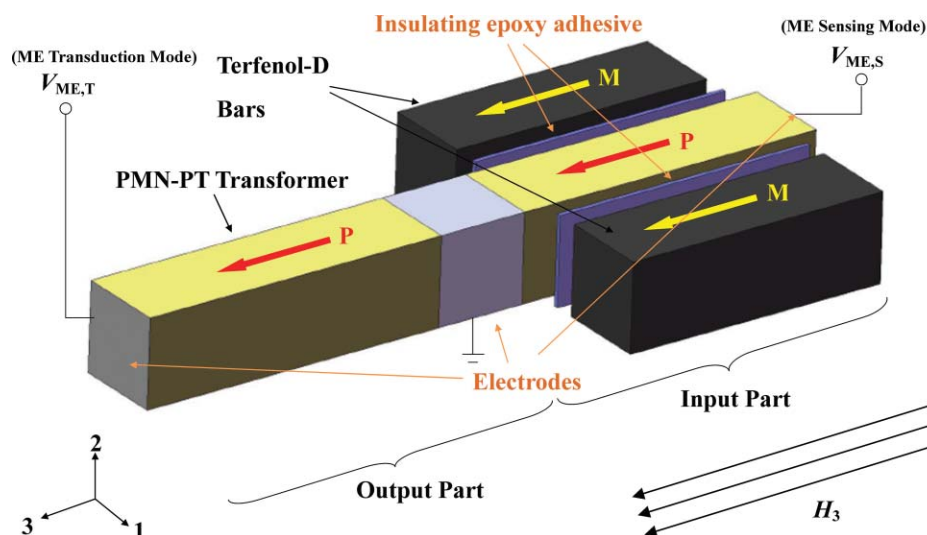


FIG. 2. (Color online) Schematic diagram of the proposed heterostructure based on a long-type PMN-PT transformer and two Terfenol-D bars. The arrows M and P indicate the magnetization direction of the Terfenol-D bars and the polarization direction of the PMN-PT transformer, respectively.

system.²⁵ The heterostructure was placed between the pole gap of a water-cooled, U-shaped electromagnet (Mylten PEM-8005K), and the electromagnet was energized by a dc current supply (Sorensen DHP200–15) to give a dc magnetic bias field (H_{Bias}). An arbitrary waveform generator (Agilent 33210A) connected to a constant-current supply amplifier (AE Techtron 7796HF) was employed to drive a pair of Helmholtz coils for providing an ac magnetic drive field (H_3) over the prescribed frequency (f) range. H_{Bias} was monitored using a Hall-effect probe connected to a Gaussmeter (F. W. Bell 7030), while H_3 was measured using a pick-up coil connected to an integrating fluxmeter (Walker MF-10D). All quantities were gathered, together with the induced ME sensor mode voltage ($V_{\text{ME,S}}$) and ME transduction mode voltage ($V_{\text{ME,T}}$), using a data acquisition unit (Nation Instruments BNC-2110 and NI-PCI6132) under the control of a computer with a Labview program. The electrical impedance ($|Z|$) and phase angle (θ) spectra of the heterostructure were measured using an impedance analyzer (Agilent 4294A).

III. RESULTS AND DISCUSSION

Figure 3 shows the electrical impedance ($|Z|$) and phase angle (θ) as a function of frequency (f) for the ME sensing mode [Fig. 3(a)] and ME transduction mode [Fig. 3(b)] of the heterostructure under open-circuit condition. For the ME sensing mode in Fig. 3(a), two obvious electromechanical res-

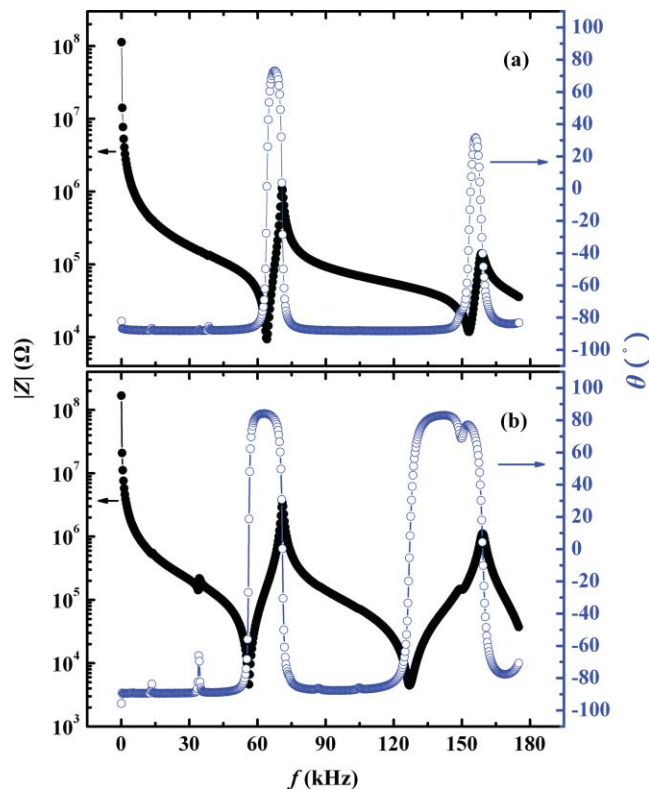


FIG. 3. (Color online) Electrical impedance ($|Z|$) and phase angle (θ) as a function of frequency (f) for (a) ME sensing mode and (b) ME transduction mode of heterostructure under open-circuit condition.

onances are observed at 64.2 and 153.4 kHz, corresponding to the first (or half-wavelength) and second (or full-wavelength) longitudinal (shape) resonances, respectively. A schematic diagram showing the displacement and stress distributions along the length of the PMN-PT transformer for these two longitudinal resonances is illustrated in Fig. 1. For the ME transduction mode in Fig. 3(b), the first and second longitudinal resonances are seen at lower frequencies of 56.1 and 127.8 kHz, respectively. These resonances are both enhanced from those of the ME sensing mode due to the piezoelectric transformer effect at resonance. Nevertheless, the clear and sharp resonances in both modes confirm the existence of good mechanical coupling between the Terfenol-D bars and the PMN-PT transformer in the heterostructure.

Figure 4 plots the frequency (f) dependence of ME voltage coefficient (α_V) at various dc magnetic bias fields (H_{Bias}) for the ME sensing mode [Fig. 4(a)] and ME transduction mode [Fig. 4(b)] of the heterostructure at an ac magnetic drive field (H_3) of 1 Oe peak. For both modes, it is found that α_V increases initially with increasing H_{Bias} , reaches their maximum values at an optimal H_{Bias} of 800 Oe, and then decreases with increasing H_{Bias} . For the ME sensing mode in Fig. 4(a), a large nonresonance α_V of ~ 0.32 V/Oe is observed in the flat f range of 1–50 kHz at $H_{\text{Bias}} = 800$ Oe. Moreover, two resonance α_V of 5.0 and 3.8 V/Oe are detected at 67.5 and 155.8 kHz, respectively. The presence of these two resonance α_V agrees

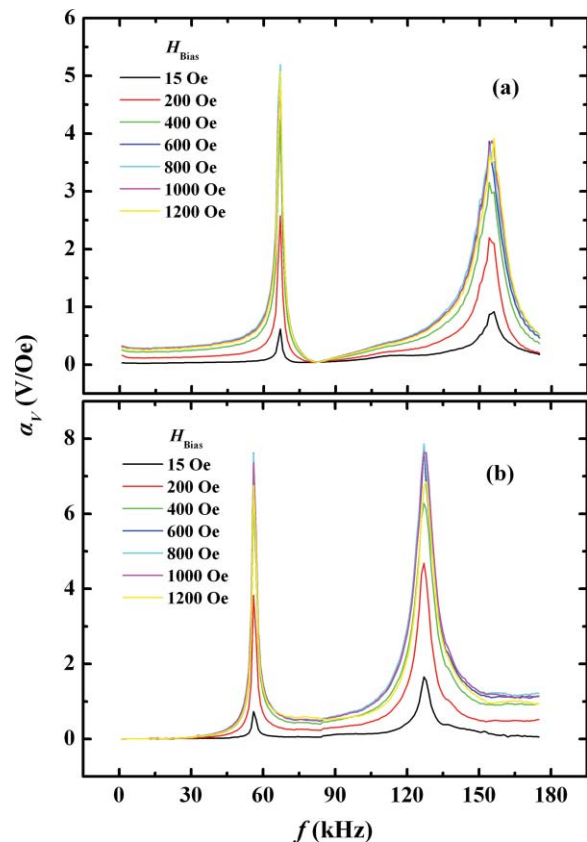


FIG. 4. (Color online) Frequency (f) dependence of ME voltage coefficient (α_V) at various dc magnetic bias fields (H_{Bias}) for (a) ME sensing mode and (b) ME transduction mode of heterostructure at an ac magnetic drive field (H_3) of 1 Oe peak.

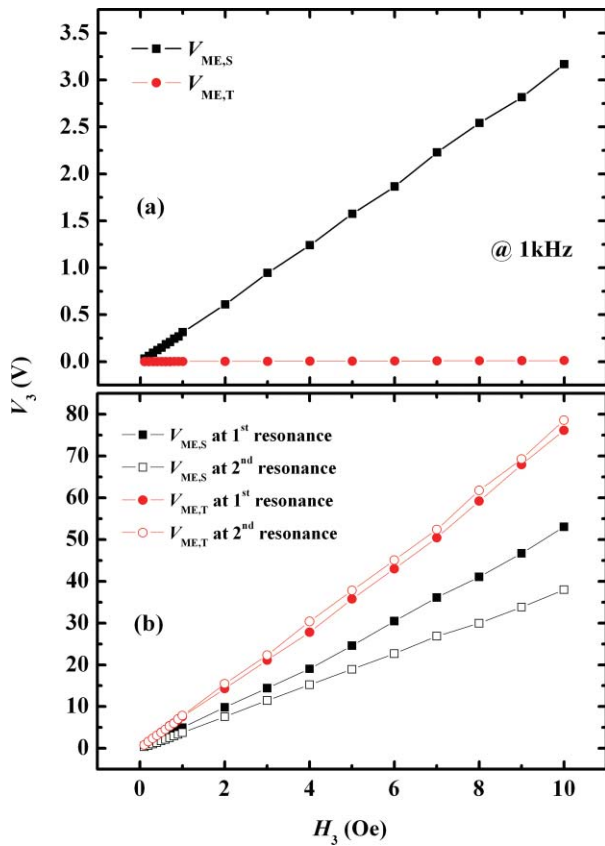


FIG. 5. (Color online) Variations of induced ME sensing mode voltage ($V_{ME,S}$) and ME transduction mode voltage ($V_{ME,T}$) on ac magnetic drive field (H_3) at an optimal dc magnetic bias field (H_{Bias}) of 800 Oe at (a) a nonresonance frequency of 1 kHz and (b) the first and second longitudinal resonance frequencies.

with that in Fig. 3(a) at 64.2 and 153.4 kHz, respectively. This agreement indicates the great contribution of the electromechanical activity to the resonance ME effect and confirms the operation of the ME sensing mode at the first and second longitudinal resonances. For the ME transduction mode in Fig. 4(b), two colossal resonance α_V of 7.6 and 7.9 V/Oe are observed at 56.2 and 127.9 kHz, respectively, at $H_{Bias} = 800$ Oe. Again, the occurrence of these two resonance α_V coincides with that in Fig. 3(b) at 56.1 and 127.8 kHz, respectively. It is noted that these colossal resonance α_V are approximately two times larger than those of the ME sensing mode in Fig. 4(a). This resonance enhancement suggests a better conversion of ME energy, and the operational mode is thus called ME transduction mode. In fact, the ME effect can further be enhanced if shielding of magnetic noise is adopted and heterostructure fabrication is improved.

Figure 5 shows the variations of induced ME sensing mode voltage ($V_{ME,S}$) and ME transduction mode voltage ($V_{ME,T}$) on ac magnetic drive field (H_3) at an optimal dc magnetic bias field (H_{Bias}) of 800 Oe at a nonresonance frequency of 1 kHz [Fig. 5(a)] and at the first and second longitudinal resonance frequencies [Fig. 5(b)]. For both the nonresonance and resonance cases, $V_{ME,S}$ and $V_{ME,T}$ exhibit linear responses to H_3 in the range of 0.1–10 Oe. For the nonresonance case in Fig. 5(a), α_V , as determined from the slope of the curve, is 320 and 1.16 mV/Oe at 1 kHz for the ME sensing mode and

ME transduction mode, respectively. For the resonance case in Fig. 5(b), α_V at the first longitudinal resonance is 5.0 and 7.6 V/Oe, while that at the second longitudinal resonance is 3.8 and 7.9 V/Oe, for the ME sensing mode and ME transduction mode, respectively. These resonance α_V are much larger than traditional laminated composites of Terfenol-D alloy and PMN-PT single crystal.¹⁰

IV. CONCLUSION

We have developed a novel heterostructure based on a long-type PMN-PT transformer and two Terfenol-D bars, and investigated its dual-mode ME effect. It has been found that the heterostructure possesses two independent operational modes, including a first ME sensing mode characterized by a large α_V of ~ 0.32 V/Oe over a flat frequency range of 1–50 kHz and a second ME transduction mode featured two colossal resonance α_V of 7.6 and 7.9 V/Oe, representing the first and second longitudinal resonances, at 56.1 and 127.3 kHz, respectively. This enhanced dual-mode ME effect makes the heterostructure great potential for advanced power-free ME sensor and transducer applications.

ACKNOWLEDGMENTS

This work was supported by the Research Grants Council of the HKSAR Government (PolyU 5266/08E). The Hong Kong Polytechnic University (4-ZZ7T), the Shanghai Normal University Program (SK201026 and PL929), the Science and Technology Commission of Shanghai Municipality (10ZR1422300), and the Innovation Program of Shanghai Municipal Education Commission (11YZ82)

¹N. A. Spaldin and M. Fiebig, *Science* **309**, 391 (2005).

²M. Bibes and A. Bathelemy, *Nature Mater.* **7**, 425 (2008).

³T. K. Chung, G. P. Carman, and K. P. Mohanchandra, *Appl. Phys. Lett.* **92**, 112509 (2008).

⁴J. Y. Zhai, Z. P. Xing, S. X. Dong, J. F. Li, and D. Viehland, *Appl. Phys. Lett.* **88**, 062510 (2006).

⁵V. J. Folen, G. T. Rado, and E. W. Stalder, *Phys. Rev. Lett.* **6**, 607 (1961).

⁶G. L. Yuan, S. W. Or, and H. L. W. Chan, *J. Appl. Phys.* **101**, 064101 (2007).

⁷G. L. Yuan, S. W. Or, H. L. W. Chan, and Z. G. Liu, *J. Appl. Phys.* **101**, 024106 (2007).

⁸G. L. Yuan, K. Z. Baba-Kishi, J. M. Liu, S. W. Or, Y. P. Wang, and Z. G. Liu, *J. Am. Ceram. Soc.* **89**, 3136 (2006).

⁹C. W. Nan, M. I. Bichurin, S. X. Dong, D. Viehland, and G. Srinivasan, *J. Appl. Phys.* **103**, 031101 (2008).

¹⁰J. Ryu, S. Priya, A. V. Carazo, K. Uchino, and H. E. Kin, *J. Am. Chem. Soc.* **84**, 2905 (2001).

¹¹S. X. Dong, J. Zhai, J. F. Li, and D. Viehland, *Appl. Phys. Lett.* **88**, 082907 (2006).

¹²Y. J. Wang, S. W. Or, H. L. W. Chan, X. Y. Zhao, and H. S. Luo, *J. Appl. Phys.* **103**, 124511 (2008).

¹³S. X. Dong, J. F. Li, and D. Viehland, *Appl. Phys. Lett.* **85**, 2307 (2004).

¹⁴Y. M. Jia, H. S. Luo, X. Y. Zhao, and F. F. Wang, *Adv. Mater.* **20**, 4776 (2008).

¹⁵Y. J. Wang, F. F. Wang, S. W. Or, H. L. W. Chan, X. Y. Zhao, and H. S. Luo, *Appl. Phys. Lett.* **93**, 113503 (2008).

¹⁶C. M. Leung, S. W. Or, S. Y. Zhang, and S. L. Ho, *J. Appl. Phys.* **107**, 09D918 (2010).

¹⁷S. S. Guo, S. G. Lu, Z. Xu, X. Z. Zhao, and S. W. Or, *Appl. Phys. Lett.* **88**, 182906 (2006).

- ¹⁸Y. J. Wang, C. M. Leung, F. F. Wang, S. W. Or, X. Y. Zhao, and H. S. Luo, *J. Phys. D.* **42**, 135414 (2009).
- ¹⁹C. A. Rosen, "Ceramic Transformer and Filters," in Proceedings of the Electronic Components Symposium (Engineering, New York, 1956), pp. 205–211.
- ²⁰K. Uchino, S. Priya, S. Ural, A. Vazquez-Carazo, and T. Ezaki, "High Power Piezoelectric Transformers—Their Applications to Smart Actuator Systems," in Proceedings of Symposium of Developments in Dielectric Materials and Electronic Devices (Am. Ceram. Soc. 2005), pp. 383–395.
- ²¹J. Hu, Y. Fuda, M. Katsuno, and T. Yoshida, *Jpn. J. Appl. Phys.* **38**, 3208 (1999).
- ²²F. Wang, W. Shi, Y. Tang, X. Chen, T. Wang, and H. Luo, *Appl. Phys. A* **100**, 1231 (2010).
- ²³H. S. Luo, G. S. Xu, P. C. Wang, H. Q. Xu, T. H. He, and W. Q. Jin, *Appl. Phys. Lett.* **85**, 6221 (2004).
- ²⁴S. X. Dong, J. F. Li, and D. Viehland, *Appl. Phys. Lett.* **85**, 5305 (2004).
- ²⁵S. W. Or, T. Li, and H. L. W. Chan, *J. Appl. Phys.* **97**, 10M308 (2008).